www.czasopisma.pan.pl PAN POLSKA AKADEMIA NAUK www.journals.pan.pl

Arch. Metall. Mater. **67** (2022), 2, 569-576

DOI: https://doi.org/10.24425/amm.2022.137792

I. VOICULESCU[1], V. GEANTA[2*], T. CHERECHES[3], P. VIZUREANU[4], R. STEFANOIU[2], A. ROTARIU[5], D. MITRICA[6]

IMPACT BEHAVIOR OF THE BALLISTIC TARGETS PACKAGE COMPOSED OF DYNEEMA POLYMER AND HIGH ENTROPY ALLOY STRUCTURES

Ballistic targets are multi-material assemblies that can be made of various materials, such as metal alloys, ceramics, and polymers. Their role is to provide collective or individual ballistic protection against high-speed dynamic penetrators or kinetic fragments. The paper presents the impact behavior with incendiary perforating bullets having 7.62 mm of ballistic packages made of combinations between Dyneema ultra-high-molecular-weight polyethylene and high entropy alloy from alloying system AlCoCrFeNi, by analyzing the dynamic phenomena (deformation, perforation) that take place at high speeds. The geometry evolution of the physical model subjected to numerical simulation allows a very good control over the discretization network and also allows the export for modeling to nonlinear transient phenomena. The results obtained by numerical simulation showed that the analyzed ballistic package does not allow sufficient protection for values of impact velocities over 500 m/sec.

Keyword: ballistic target; high entropy alloy; Dyneema polymer; impact; numerical simulation

1. Introduction

Armor has long been a method used to protect people involved in defense actions or on the battlefield. Concerns about the manufacture of the most resistant and efficient armor are still very relevant today. The basic conditions of an optimized armor are capacity to absorb and redistribution the impact energy, in order to diminish the force per unit area of armor material, to stop the penetrating bullets or cutting/breaking some of them, and compressing layers of fibers ahead of it [1]. To ensure the optimal conditions for the manufacture of ballistic protection equipment, military and security specifications have been developed, which provide for test procedures, protection levels provided according to impact speeds with different types of penetrators, environmental conditions and characteristics of materials used (minimum 540-600 BHN or 55-60 Rockwell C, minimum yield and tensile strength 1500 to 1700 MPa, minimum transverse Charpy-V impact energy of 13 J at –40°C and minimum elongation of 6%) [2,3]. Considering these required properties, more of armors have been realized by metallic alloys: high strength low-carbon martensitic steel [3], high strength steel [4], high entropy alloys from AlCoCrFeNi alloying system [5-7], Weldox 700E steel [8], AISI 4340 Q&T steel [9-11], 500 HB high hardness armor steel [12].

Recently, a series of organic materials, such as laminated woven bamboo [13] or pineapple fibers [14] were integrated into E-glass unsaturated polyester or associated with Kevlar, for improve the impact and wear behavior. Lately, systems composed of several types of materials (metallic, ceramic, polymeric) are used to exploit their properties of mechanical strength, low density, impact energy absorption capacity. Thus, various types of ballistic packages composed of combinations of metal plates (titanium alloys from the Ti_6Al_4V system [15]), and highly elastic ultra-high molecular weight polyethylene (UHMWPE), Polycarbonate [16], Polymers and Fibre-Reinforced Plastics [17], SiC / UHMWPE [18], Kevlar fabric impregnated with n-SiO_2 / PEG mixtures [19] and Kevlar 706 Greige fabric (CS-811 finish) [20], Twaron fabrics and Dyneema UD laminates [21], alumina (Al_2O_3) containing 4 wt.% of (Nb_2O_5) [22]. Carbon fibers can also be processed to obtain the desired strength. The

[1] UNIVERSITY POLITEHNICA OF BUCHAREST, FACULTY OF INDUSTRIAL ENGINEERING AND ROBOTICS, 060042 SPLAIUL INDEPENDENTEI 313, BUCHAREST, ROMANIA
[2] UNIVERSITY POLITEHNICA OF BUCHAREST, FACULTY OF MATERIALS SCIENCE AND ENGINEERING, 060042 SPLAIUL INDEPENDENTEI 313, BUCHAREST, ROMANIA
[3] UPS PILOR ARM, LAMINORULUI STREET, 2, TARGOVISTE, ROMANIA
[4] GHEORGHE ASACHI TECHNICAL UNIVERSITY OF IASI, FACULTY OF MATERIALS SCIENCE AND ENGINEERING, 67, DIMITRIE MANGERON STREET, ROMANIA
[5] MILITARY TECHNICAL ACADEMY FERDINAND I, 050141, GEORGE COSBUC, 39-49, BUCHAREST, ROMANIA
[6] NATIONAL RESEARCH-DEVELOPMENT INSTITUTE FOR NON-FERROUS AND RARE METALS – IMNR, 077145, BIRUINTEI, 102, PANTELIMON, ROMANIA

* Corresponding author: victorgeanta@yahoo.com

different types of carbon fiber differ in flexibility, electrical, thermal conductivity and chemical resistance. Carbon fibers coated with a layer of boron have special mechanical properties. However, the extremely high costs of these types of materials limit their use only to high temperature applications [23].

Polyethylene fibers have a mechanical strength 10 times higher than steel and up to 40% higher than aramid fibers. Polyethylene fibers are also very light, resistant to water and chemical agents. They are used in many applications, including bulletproof vests, helmets, armored vehicles, protective equipment. The impact behavior of the new multi layered ballistic package was good enough to be considered an alternative to replace expensive Kevlar laminates [24].

Recent studies [25] have been dedicated to improve the protection to conventional level IIIA of ballistic armor vests, by introducing the PALF composite plate (natural fibers extracted from pineapple leaves). The impact tests, performed with 7.62 mm caliber ammunition on this new type of ballistic armor, exhibited a back-face signature depth of 26.6 mm, which meets the NIJ standard for ballistic protection (smaller than 44 mm).

Due to the fact that the impact resistance is a critical property for the ballistic package, both numerical simulation studies and impact tests using incendiary bullet must be performed before approval of new protection system [26-28].

In this paper impact tests performed with incendiary perforating bullets of 7.62 mm caliber against ballistic package containing high entropy alloy from alloying system AlCoCrFeNi and Dyneema ultra-high-molecular-weight polyethylene are presented. The dynamic phenomena (deformation, perforation) that take place at high speeds were studied using the physical model subjected to numerical simulation. The results obtained by numerical simulation were completed with real tests performed with 7.62 mm caliber ammunition, in the ballistic tunnel, in order to determine the protection level for different values of impact velocities.

purity). The electric arc for melting was primed between the tungsten electrode (alloyed with 2% Th) and the metallic materials placed on the melting copper plate. The metallic ingots were rotated and remelted 5 times on each side to improve chemical homogeneity [26-28].

Nine round plates with a diameter of 65 mm and thickness of 8 mm were used for impact testing. As results from Fig. 1, the samples surfaces in as-cast state was covered with a thin layer of complex oxide, which must be removed by cutting [26]. Cutting behavior of HEA from AlCoCrFeNi system is better than those of stainless steels (59% easier to perform cutting of plate surface). An important aspect that appears during cutting of such HEA is the self-hardening effect, caused mainly by the cutting force components [29].

Fig. 1. As-cast HEA samples from AlCoCrFeNi alloying system

2. Experiment

2.1. Materials and methods

The first stage of the experimental program was to obtain plates from alloys with high entropy. The alloy used in the study was selected following mechanical and ballistic tests performed under standard conditions. The high entropy alloy (HEA) used in the experimental program was $Al_{0.6}CrFeCoNi$ (aluminum atomic ratio $x = 0.6$). This alloy contains 5 different chemical elements, as follows: 6.16wt% Al; 24.36wt% Co; 21wt% Cr; 23.12wt% Fe and 24.36wt% Ni. The metallic alloy was obtained by melting in VAR ABJ 900 equipment, in ERAMET Laboratory from University Politehnica of Bucharest, Romania. The technical purity raw materials (99.5%) used for the HEA obtaining were placed on the melting plate as granules with diameter of 2 to 5 mm. The melting was performed with electric energy under a protective atmosphere with argon (99.9%

The mechanical properties and stability of the microstructure were improved by annealing at 700°C/4 hours followed by air cooling (TT1 treatment), then aging at 1100°C/2 h followed by air cooling (TT2 treatment) in Nabertherm LT 15/12 / P320 furnace, having a programmable system for setting the thermal regime. The different heat treatments determine the modification of the hardness and the morphology of the phases in the high entropy alloys [30-33].

The microstructure of the alloy was analyzed using Inspect S SEM microscope equipped with EDAX analyzer Z2e and by using Olympus GX 51 optical microscope equipped with AnaliSYS software for images processing. Before the metallographic preparation, the specimens cut from HEAs (as-cast, heat treated) were hot embedded in PhenoCure resin (pressure of 5 bars and temperature of 185°C). Then, the specimens surfaces were metallographic polished using abrasive paper (grit 400-1200) and polished, using alpha alumina (grit of 3 to 0.1 μm). After that, the specimen surfaces were cleaned with isopropyl alcohol and

then were electrochemically etched in 10% oxalic acid, (0.06A and 3V, for 2 minutes).

The phase compounds of the $Al_{0.6}CoCrFeNi$ alloy has been identified in our previous study [34]. Using XRD method has been identified the microstructure of this high entropy alloy that contains both BCC and FCC phases, with the crystallites size of 23.96 nm [34]. The hardness of HEA (in as-cast state and after the heat treatments succession) was measured using Shimadzu HMV 2T apparatus, by setting the testing force values of 1.961 N and loading time of 10 seconds. The tensile tests have been performed using „W+b" Walter + bai ag testing machine. The thickness value of as-cast plates was reduced to 6 mm by grinding process. After dimensional adjustment, HEA plates were inserted into the ballistic packages to be dynamically tested.

2.2. Physical model

The ballistic packages studied in the paper were made of metal plates (Al and high entropy alloy × HEA) and Dyneema plate (Fig. 2a). The placement order within the ballistic package was established according to the role of each material. Thus, the succession of materials was: first impacted plate was made of aluminum with 2 mm thickness (its role was to support the other components in the ballistic package), the next plate was made of HEA with 6 mm thickness (with role of reducing the impact speed of the penetrator), the 3rd plate was made of Dyneema with 10 mm thickness (with the role of absorbing the impact energy) and the last plate was also made of aluminum with 2 mm thickness (with the role of sealing the ballistic package).

The package was then introduced in an aluminum frame for mechanically rigidizing, and then all this assembly was impregnated with phenolic resin, with the role of stiffening and immobilizing the components (Fig. 2b).

The geometry of the physical model subjected to the simulation was designed using the COSMOS program that allows a very good control over the discretization network and allows the export to LS-DYNA, a specialized program in modeling nonlinear transient phenomena.

2.3. Ballistic tests

In order to validate the results obtained by numerical simulation, a series of practical tests were performed in the specialized laboratory of the Military Technical Academy in Bucharest. The ballistic box containing plates made by different materials (Al, HEA and Dyneema, Figure 3a) was impacted with incendiary bullet of 7.62 mm caliber, fired with a machine gun.

The maximum bullet launch speed (695 m/s) was chosen to verify compliance and to validate the physical model, based on the average value of the bullet velocity reached in real conditions (in ballistic tunnel). The ballistic boxes assembled and impregnated with resin were fixed on a wooden panel using 2 screws, their positioning being made so that they are placed on the firing axis of the machine gun (Fig. 3b). After each firing, the boxes were detached from the wood panel and the perforation effects on impact with the dynamic penetrator were analyzed.

3. Results and discussion

3.1. Materials characteristics

High entropy alloys from AlCoCrFeNi system have atypical behaviors during heat treatments. Depending on chemical composition, the softening can occurs after aging, being caused by the slow transformations at high temperatures. In slow cooling conditions, the wear resistance can be higher compared to the steel, even if hardness is lower. This surprising effect was explained by Yeh [32] and is determined by the occurrence of ρ phases during homogenization at 1100°C [32-33]. Microstructure of HEA (OM – optical microscopy, SEM – scanning electron microscopy) in as-cast state and after heat treatments is shown in Fig. 4.

The morphology of the grains was successively transformed from coarse dendrites (Fig. 4a) into partially decomposed and rounded particles (during annealing, Fig. 4b), then a multitude of small inter-metallic compounds are separated from the base matrix (during aging, Fig. 4c).

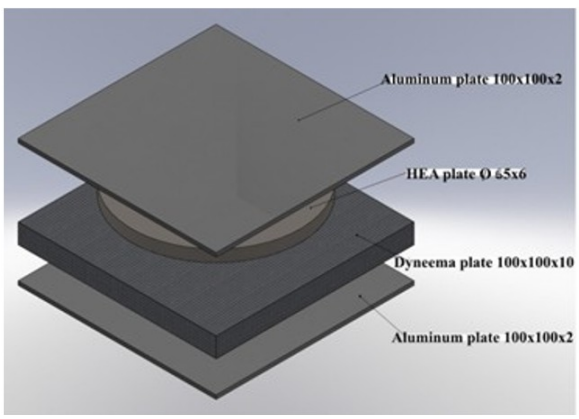

a) The components of the ballistic package

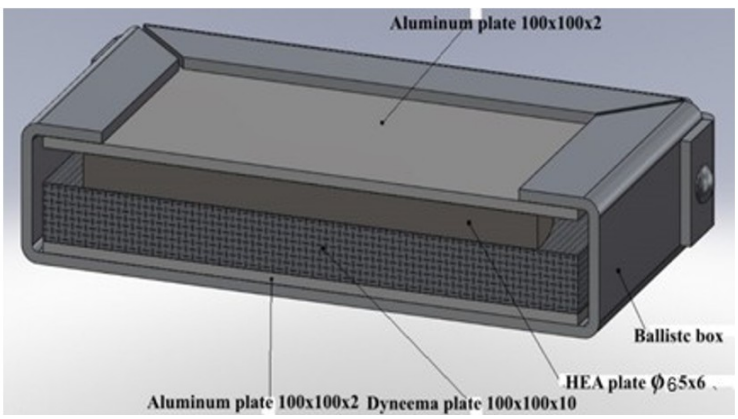

b) Cross section by assembly of ballistic box

Fig. 2. Ballistic package

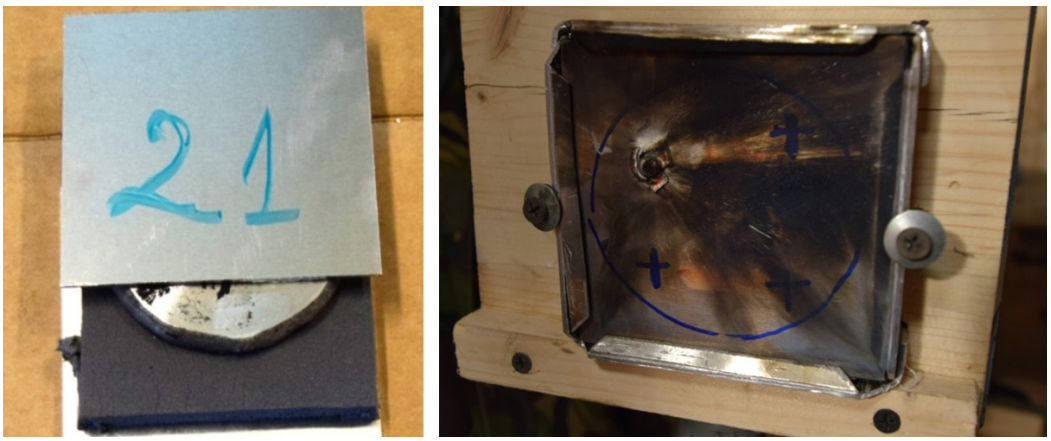

Fig. 3. The component elements of the ballistic box and the fixing mode for firing

This behavior influenced the hardness properties. It has been found that the metallic matrix become more soften, as a result of recovery, recrystallization and precipitation of intermetallic phases that appears after long-term aging treatment (72 hours). This treatment allows to increasing the impact energy during Charpy tests performed at 20°C (from 62 J in as-cast state to 68 J after heat treatment TT2).

The average microhardness has increase from 245 $HV_{0.2}$ in as-cast state to 403 $HV_{0.2}$ after annealing at 700°C/4 h/air, then decrease to 379 $HV_{0.2}$ after annealing at 700°C/4 h/air + aging at 1100°C/2 h/air. In the same time, after annealing the compression strength has increased from 2635 MPa to 2919 MPa.

Before being incorporated into ballistic packages, HEA plates were struck with incendiary perforating projectiles to estimate their protective capacity. The heat treatments efficiency could be observed by the ability of the material to stop the bullet in the metallic wall (Fig. 5). Prior to the heat treatment, the bullet pierced and broke the metallic wall (Fig. 5a). After annealing + aging, the bullet could not completely pierce the metal wall, remaining stuck in it (Fig. 5b).

3.2. Numerical simulation

The impact behavior of the materials involved in the simulation (from the simplest with linear elastic behavior, to the most complex, like Johnson-Cook type), was estimated by equations that include a series of material coefficients [27-28]. In this study, the material coefficients for the high entropy alloy were determined experimentally, while for the other materials the values

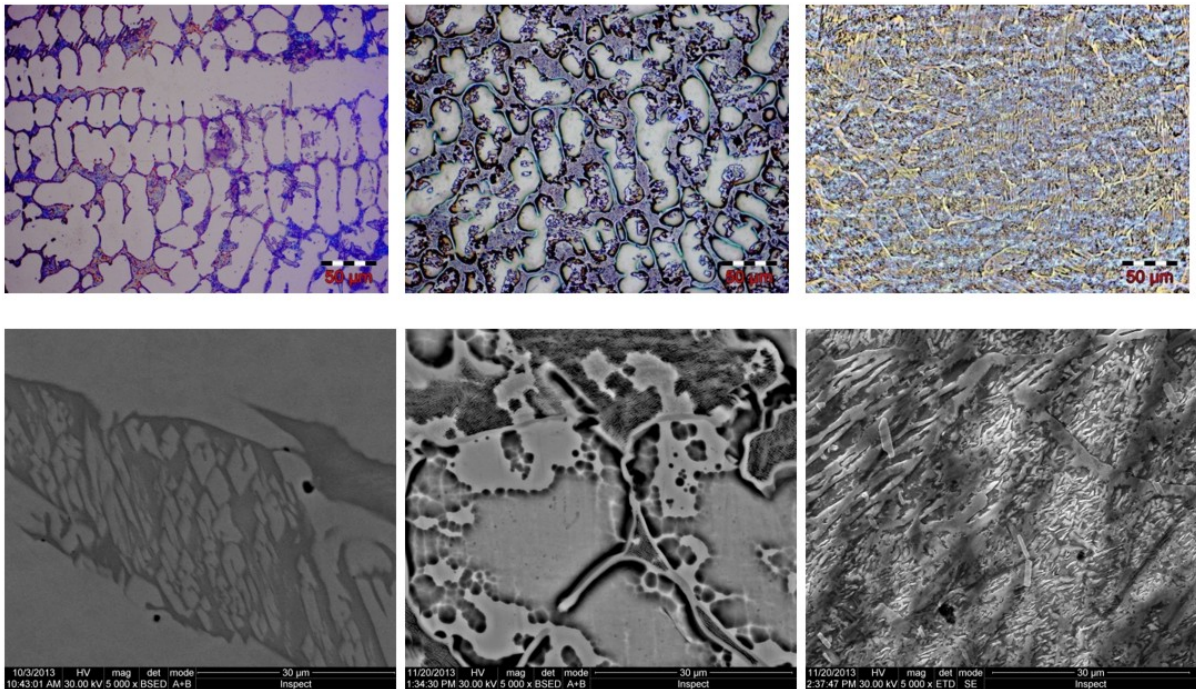

a) b) c)

Fig. 4. HEA microstructure in different processing stages (OM – up; SEM – down). a) as cast; b) annealed at 700°C/4 h/air; c) annealed at 700°C/4 h and ageing at 1100°C/2 h/air

a) b)

Fig. 5. The impact behaviour of HEA plates before and after heat treatment

from the literature were used. For the numerical simulation of the impact processes of the multi-material ballistic package with kinetic penetrators, the finite element method was used. This method uses a graphical representation of a Lagrange material network, which is associated with the bodies and which deforms together with them. In the three successive images generated by the finite element program, the hole produced by the 7.62 mm caliber bullet that passed through the materials in the ballistic box can be seen. The mechanical characteristics of the most important materials (bullet core and HEA) that have been included in the physical model designed for the numerical simulation of the ballistic boxes impacted with the incendiary bullet having a caliber 7.62 mm, are indicated in TABLE 1.

TABLE 1

Materials properties and Johnson-Cook coefficients

Properties	HEA Al0.6CoCrFeNi	Bullet core
Density, Kg/m^3	7720	7850
Transverse modulus of elasticity, *G*, MPa	0.81×10^5	0.82×10^5
Young modulus, *E*, MPa	2.2×10^5	2.1×10^5
Poisson coefficient,	0.35	0.3
Johnson-Cook coefficients		
***A*, MPa**	1550	2800
***B*, MPa**	1200	850
n	0.24	0.18
C	0.032	0.015
m	1.00	1.00
T_{melt}, K	1850	1763
T_0, K	300	300

In the simulation program, the bullet was launched with speed of 750 m/s, this being the maximum speed that this ammunition reaches when firing with machine gun. The physical model used for the numerical simulation contain 2 aluminum plates, one HEA plate and one Dyneema (Fig. 6).

Upon impact with HEA, the bullet caused the cracks initiation and then fragmentation, resulting in a larger hole diameter. Then, on impact with Dyneema, the delamination and rupture of the fabric occurred (Fig. 7).

It can be seen that on impact with the HEA, the initial sharp tip of the bullet begins to flatten and fragment, its small fragments being scattered in the vicinity of the ballistic box exit area. Another suggestive representation, in cross section through the ballistic box, is presented in Fig. 8. Here you can see the effects that the bullet produces when passing through the materials of the ballistic package: first is perfect perforation of the frontal aluminum plate; in second stage perforation and tearing of HEA

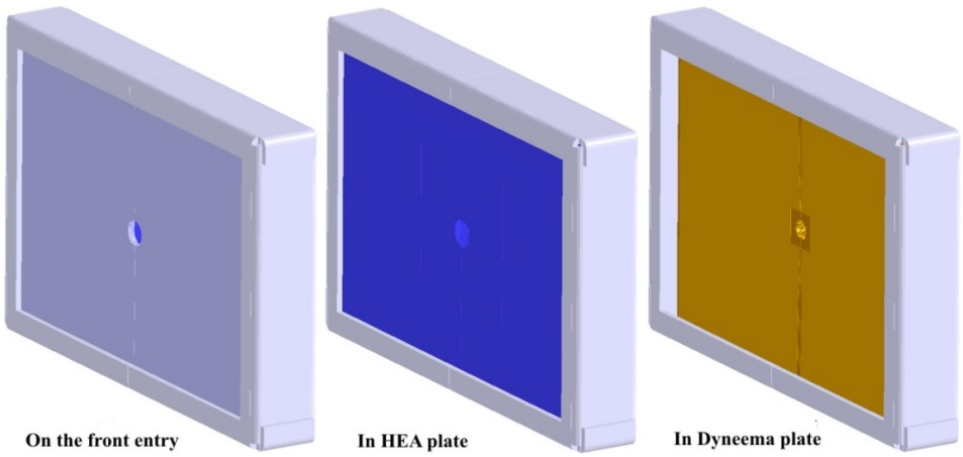

Fig. 6. Physical model (Al+HEA+ Dyneema+Al) involved in numerical simulation

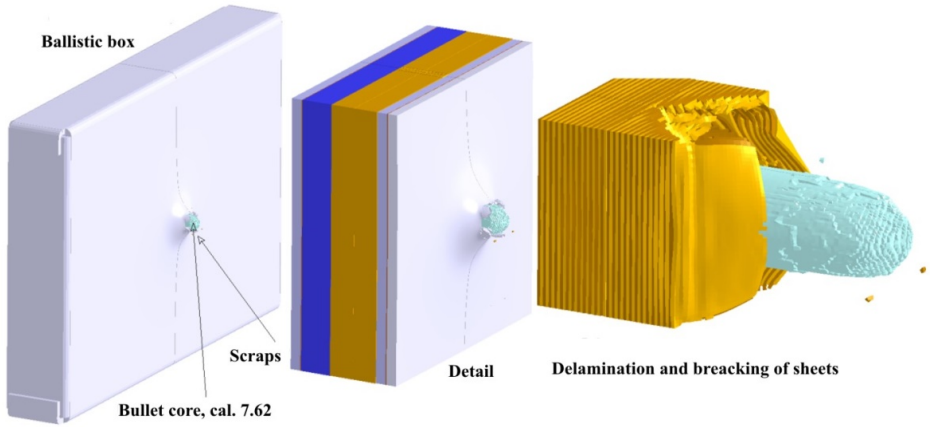

Fig. 7. Aspects of the ballistic penetration stages

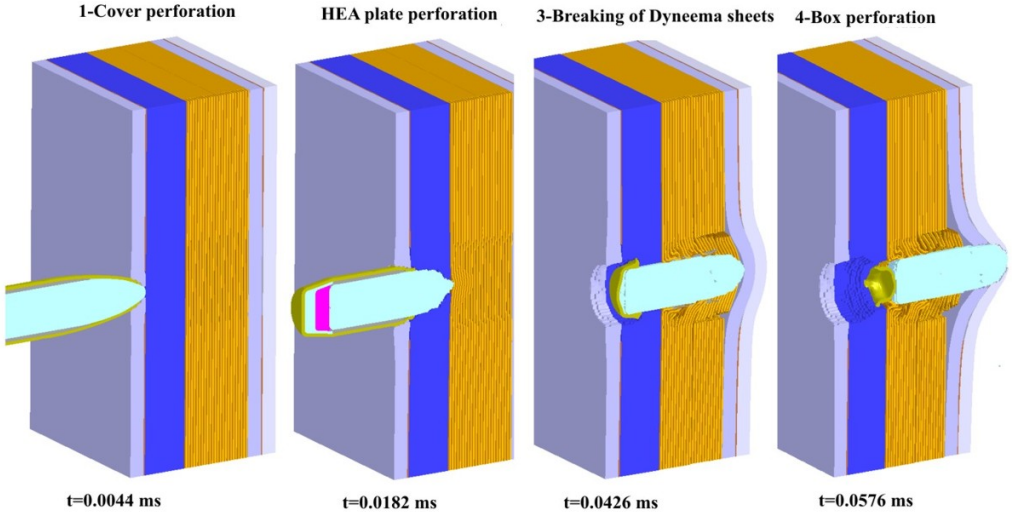

Fig. 8. The sequences during bullet penetration through ballistic package

is carried out followed by third stage, when deformation and delamination of the Dyneema plate occur; in final fourth stage the deformation and partial perforation of the last aluminum plate is carried out. As shown in the graph from Fig. 9, both the penetration velocity and the bullet energy register an accelerated decrease at the impact with HEA plate, thus highlighting the importance of this material in the ballistic package.

In the dynamic impacting process, the most important parameters are the speed of the penetrator and its kinetic energy. The time variation curves of these parameters are shown in Fig. 9.

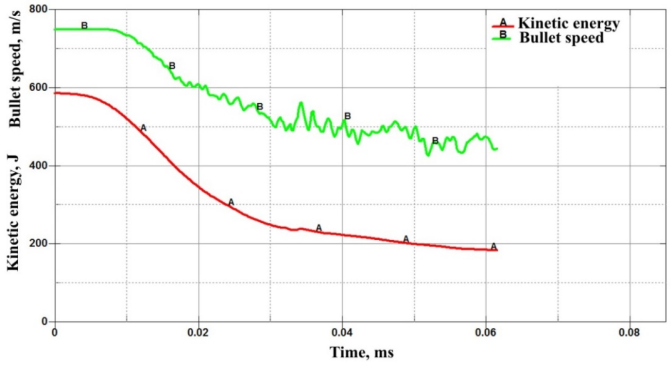

Fig. 9. Kinetic energy and penetrator speed evolution during penetration process

3.3. Firing tests

The test equipment used for ballistic evaluation must meet the all requirements for firing. The components of the testing system used for experiments were: firing table with weapon fixing system, chronograph and camera ultra-fast filming system (for measuring the bullets speed), analytical balance (for dosing the ammunition powder), thermometer and weather station (for environmental conditions measuring), calipers, computer and telescope (for adjusting impact accuracy). To ensure the appropriate ballistic impact, the testing system was set for satisfying the following conditions: the impact speed measuring tolerance of ±20 m/s compared to the nominal value; impact angle tolerance of ±0.50º in rapport with the firing system axe; firing angle tolerance of 3º or 5º; distance from the impact point to the edge or between the impact points of 25 mm (for protection levels 1-3).

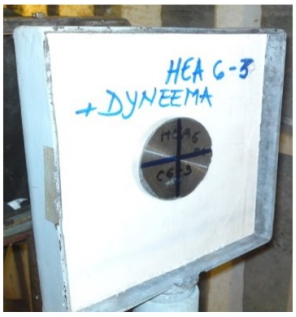

a) **Target system**

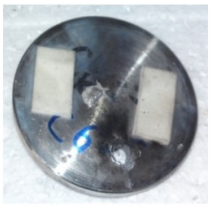

b) **Untreated HEA**
V = 434 - 469m/s
m= 1.05g
Perforated box,
Unaffected bullet

c) **Heat treated TT1**
V = 440 m/s, m = 1.05g
V = 537 m/s, m=1.20g
Perforated box, HEA plate broken, bullet partially broken

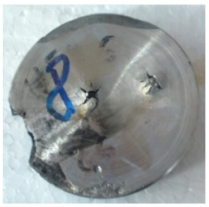

d) **Heat treated TT2**
V = 496 m/s, m=1.10g
No perforation
of ballistic box,
blocked bullet

Fig. 10. Positioning the ballistic box in the firing system and aspect of HEA impacted surface, where: V is the impact speed and m is the ammunition powder mass

The firing conditions were: temperature of 15°C, humidity of 60%, incendiary bullet type 7.62×39 mm caliber, mass of 7.67 g and mass core of 4 g.

The ballistic box was placed on the rigid support of the firing system (Fig. 10a), then 2 successive incendiary bullets were fired for each ballistic package, being made a total of 18 shots for the analyzed materials combination. Each ballistic box was coded for impact behavior analysis with different impact velocity values. After performing the firing program, the impact surfaces of HEA were analyzed and conclusions were drawn regarding the degree of protection provided by the combination of materials used in the study (Figs 10b, 10c and 10d).

The impact speed is influenced by the quantity of ammunition mass of each bullet shirt. As the ammunition mass increase, the impact speed is greater. For similar impact speed values, the untreated samples were completely perforated and the bullet tip was unaffected by the impact with the target. In the case of HEA heat treated TT1, the bullet tip was partially broken and the metallic plates were perforated and broken. A good effect is, in this situation, reduction of perforation capacity of bullet tip. As result from data presented in figure 10, the best results were obtained in the case of samples HEA heat treated TT2. In this case, the plates were partially perforated and the bullet was retained in the metallic wall.

For comparison, some armored steel plates were tested under the same conditions as the experimental HEA plates. The behavior of the armor steel was good for impact velocity below 450 m/s. For higher impact velocity values (491 m/s), the armor steel plate was completely perforated, without any influence on the bullet tip. The role of Dyneema plates in this type of ballistic target was minor. If the HEA plates have been partially perforated, then broken fragments from HEA or from bullet can be retained in the Dyneema plate.

4. Conclusions

High entropy alloy from AlCoCrNiFe alloying system can be a possible candidate for fabrication the protective metallic walls in military applications. For the same impact speed values of the dynamic projectile, heat treated HEA from the alloying system $Al_{0.6}CoCrNiFe$ has a better capacity to retain the bullet than armor steel.

Dyneema plates cannot have the same dynamic impact performance as the high entropy alloys from $Al_{0.6}CoCrNiFe$ alloying system. At best, they can be used as final plates to retain debris and broken fragments from materials of target or bullets. The main advantage of Dyneema boards is that they have a lower density than HEA and contribute to the reducing total mass of the protective wall.

Both the penetration velocity and the bullet energy register an accelerated decrease at the impact with HEA plate, thus highlighting the importance of this material in the ballistic package.

Acknowledgments

The research work was financially supported by the Romanian Ministry of Research and Innovation, CCCDI – UEFISCDI, project number PN-III-P1-1.2-PCCDI-2017-0239/20 PCCDI 2018, "Individual and collective protection systems for the military domain based on high entropy alloy – HEAPROTECT" and project number PN-III-P2-2.1-PED-2019-3953, contract 514PED/2020 "New ceramic layer composite material processed by laser techniques for corrosion and high temperature applications – LASCERHEA", within PNCDI III.

REFERENCES

[1] G. Cooper, Ph. Goots, Ballistic Protection: Chapter IV, 2003 British Crown copyright 2003/DSTL.

[2] https://www.grandviewresearch.com/industriy-analysis/military-personal-protective-equipment-market

[3] K. Maweja, W. Stumpf, The design of advanced performance high strength low-carbon martensitic armour steels. Microstructural considerations, Materials Science and Engineering **A 480**, 160-166 (2008).

[4] P.K. Jena, K.S. Kumar, V.R. Krishna, A.K. Singh, T.B. Bhat, Studies on the role of microstructure on performance of a high strength armour steel, Engineering Failure Analysis **15**, 1088-1096 (2008).

[5] V. Geanta, T. Chereches, P. Lixandru, I. Voiculescu, R. Stefanoiu, D. Dragnea, T. Zecheru, L. Matache, Virtual Testing of Composite Structures Made of High Entropy Alloys and Steel, Metals **7** (11), 496 (2017).

[6] V. Geanta, I. Voiculescu, R. Stefanoiu, T. Chereches, T. Zecheru, L. Matache, A. Rotariu, Dynamic Impact Behaviour of High Entropy Alloys Used in the Military Domain, Conference Series-Materials Science and Engineering (374), UNSP 012041 (2018).

[7] L.C. Matache, P. Lixandru, T. Chereches, A. Mazuru, D. Chereches, V. Geanta, I. Voiculescu, E. Trana, A.N. Rotariu, Determination of material constants for high strain rate constitutive model of high entropy alloys, MODTECH 2019. IOP Conference Series-Materials Science and Engineering (591), 012057 (2019).

[8] E. Palta, M. Gutowski, H. Fang, A numerical study of steel and hybrid armor plates under ballistic impacts, International Journal of Solids and Structures (136-137), 279-294 (2018).

[9] B.M. Balasubramanian, V., M.G. Reddy, Effect of hardfaced interlayer thickness on ballistic performance of armour steel welds, Materials and Design (44), 59-68 (2013).

[10] S. Babu, V. Balasubramanian, M.G. Reddy, T.S. Balasubramanian, Improving the ballistic immunity of armour steel weldments by plasma transferred arc (PTA) hardfacing, Materials and Design (31), 2664-2669 (2010).

[11] M. Balakrishnan, V. Balasubramanian, M.G. Reddy, K. Sivakumar, Effect of buttering and hardfacing on ballistic performance of shielded metal arc welded armour steel joints. Materials and Design (32), 469-479 (2011).

[12] N. Kılıc, B. Ekici, Ballistic resistance of high hardness armor steels against 7.62 mm armor piercing ammunition, Materials and Design (44), 35-48 (2013).

[13] A. Ali, R. Adawiyah, K. Rassiah, W. Kuan Ng, F. Arifin, F. Othman, M.S. Hazin, M.K. Faidzi, M.F. Abdullah, M.M.H. Megat Ahmad, Ballistic impact properties of woven bamboo-woven E-glass-unsaturated polyester hybrid composites, Defence Technology (15), 282-294 (2019).

[14] T. Singh, C.I. Pruncu, B. Gangil, V. Singh, G. Fekete, Comparative performance assessment of pineapple and Kevlar fibers based friction composites, J. Mater. Res. Technol. **9** (2), 1491-1499 (2020).

[15] W. Liu, Z. Chen, Z. Chen, X. Cheng, Y. Wang, X. Chen, J. Liu, B. Li, S. Wang, Influence of different back laminate layers on ballistic performance of ceramic composite armor, Materials and Design (87), 421-427 (2015).

[16] Q.H. Shah, Impact resistance of a rectangular polycarbonate armor plate subjected to single and multiple impacts, International Journal of Impact Engineering (36), 1128-1135 (2009).

[17] I.G. Crouch, Body armour – New materials, new systems, Defence Technology (15), 241-253 (2019).

[18] Z. Shen, D. Hu, G. Yang, X. Han, Ballistic reliability study on SiC/UHMWPE, composite armor against armor-piercing bullet, Composite Structures (213), 209-219 (2019).

[19] R. Pastore, G. Giannini, R.B. Morles, M. Marchetti, D. Micheli, Impact Response of Nanofluid-Reinforced Antiballistic Kevlar Fabrics, IntechOpen (2012). DOI: http://dx.doi.org/10.5772/50411

[20] G. Nilakantan, S. Horner, V. Halls, J. Zheng, Virtual ballistic impact testing of Kevlar soft armor: Predictive and validated finite element modeling of the V0-V100 probabilistic penetration response, Defence Technology (14), 213-225 (2018).

[21] Y. Yang, X. Chen, Investigation on energy absorption efficiency of each layer in ballistic armour panel for applications in hybrid design, Comp. Struct. (164), 1-9 (2017).

[22] F.O. Braga, F.S. da Luz, S.N. Monteiro, E.P. Lima Jr., Effect of the impact geometry in the ballistic trauma absorption of a ceramic multilayered armor system, J. Mater. Res. Technol. **7** (4), 554-560 (2018).

[23] A. Badakhsh, W. Han, S.C. Jung, K.H. An, B.J. Kim, Preparation of Boron Nitride-Coated Carbon Fibers and Synergistic Improvement of Thermal Conductivity in Their Polypropylene-Matrix Composites, Polymers **11**, (12) 2009.

[24] M.S. Oliveira, F.C.G. Filho, A.C. Pereira, L.F. Nunes, F. Santos da Luz, F.O. Braga, H.A. Colorado, S.N. Monteiro, Ballistic performance and statistical evaluation of multilayered armor with epoxy-fique fabric composites using the Weibull analysis, J. Mater. Res. Technol. **8** (6), 5899-5908 (2019).

[25] F. Santos da Luz, F. da Costa Garcia Filho, M. Souza Oliveira, L.F. Cassiano Nascimento, S. Neves Monteiro. (2020). Composites with Natural Fibers and Conventional Materials Applied in a Hard Armor: A Comparison, Polymers (12) (1920). DOI: https://doi.org/10.3390/polym12091920

[26] T. Chereches, P. Lixandru, V. Geanta, I. Voiculescu, D. Dragnea, R. Stefanoiu, Layered Structures Analysis, with High Entropy Alloys, for Ballistic Protection, Applied Mechanics and Materials (809-810), 724-729 (2015).

[27] V. Geanta, I. Voiculescu, T. Chereches, T. Zecheru, L. Matache, A. Rotariu, Behavior to Dynamic Loads of Composite Multi-layer Structures. Mat. Plast. Bucharest 6 (2), 460-465 (2019).

[28] V. Geanta, I. Voiculescu, Characterization and Testing of High Entropy Alloys from AlCrFeCoNi System for Military Applications, Engineering Steels and High Entropy-Alloys, p. 139-156 (2019). IntechOpen. DOI: http://dx.doi.org/10.5772/intechopen.88622

[29] G. Constantin, E. Balan, I. Voiculescu, V. Geanta, V. Craciun, Cutting behavior of Al0.6CoCrFeNi High Entropy Alloy, Materials **13** (18), 4181 (2020). DOI: https://doi.org/10.3390/ma1318418

[30] I. Voiculescu, V. Geanta, M. Ionescu, Effects of heat treatments on the microstructure and microhardness of AlxCrFeNiMn alloys. Annals of "Dunarea de Jos" University of Galati. Fasc. XII, Welding Equipment and Technology (26), 5-11 (2015).

[31] L.H. Wen, H.C. Kou, J.S. Li, H. Chang, X.Y. Xue, L. Zhou, Effect of aging temperature on microstructure and properties of CoCrCuFeNi high-entropy alloy, Intermetallics (17), 266-269 (2009).

[32] C.W. Tsai, Y.L. Chen, M.H. Tsai, J.W. Yeh, T.T. Shun, S.K. Chen, Deformation and aging behaviors of high-entropy alloy Al0.5CoCrCuFeNi, J. All. Comp. (486), 424-435 (2009).

[33] Y.F. Kao, T.J. Chen, S.K. Chen, J.W. Yeh, Microstructure and mechanical property of as-cast, -homogenized, and-deformed AlxCoCrFeNi ($0 \leq x \leq 2$) high-entropy alloys, J. All. Comp. 1-9 (2009). DOI: https://doi.org/10.1016/J.jallcom.2009.08.090

[34] V. Geantă, I. Voiculescu, I. Miloșan, B. Istrate, I.M. Mateș, Chemical Composition Influence on Microhardness, Microstructure and Phases Morphology of AlxCrFeCoNi High Entropy Alloys, Rev. chim. Bucharest **69** (4). 798-801 (2018).